Separation and Purification Technology 163 (2016) 206–214

Contents lists available at ScienceDirect

Separation and Purification Technology

journal homepage: www.elsevier.com/locate/seppur

Molecularly imprinted polymer strategies for removal of a genotoxic impurity, 4-dimethylaminopyridine, from an active pharmaceutical ingredient post-reaction stream

Teresa Esteves [a], Raquel Viveiros [b,c], João Bandarra [c], William Heggie [c], Teresa Casimiro [b], Frederico Castelo Ferreira [a,*]

[a] iBB-Institute for Bioengineering and Biosciences, Department of Bioengineering, Instituto Superior Técnico, Universidade de Lisboa, Avenida Rovisco Pais, 1049-001 Lisbon, Portugal
[b] LAQV-REQUIMTE, Departamento de Química, Faculdade de Ciências e Tecnologia, FCT, Universidade NOVA de Lisboa, 2829-516 Caparica, Portugal
[c] Hovione FarmaCiencia SA, R&D, Sete Casas, 2674-506 Loures, Portugal

ARTICLE INFO

Article history:
Received 22 December 2015
Received in revised form 29 January 2016
Accepted 30 January 2016
Available online 24 February 2016

Keywords:
Molecularly imprinted polymer
Genotoxic impurity
Active pharmaceutical ingredient purification
4-Dimethylaminopyridine
Mometasone furoate

ABSTRACT

Molecularly imprinted polymers (MIPs) are prepared and evaluated for the effective removal of the genotoxic impurity (GTI), 4-dimethylaminopiridine (DMAP), from a Mometasone furoate (Meta) solution, used as a case study relevant for the pharmaceutical industry. The MIPs formation by bulk polymerization is assessed considering different temperature regimes as well as stoichiometry of template, functional monomer, cross-linker, respectively DMAP, methacrylic acid and ethylene glycol dimethacrylate. A design of experiment (DoE) is performed to establish conditions for a maximum GTI specific binding percentage, validated experimentally at a value of 98% for 5.03 mgGTI/gMIP, for a 256 ppm GTI solution. The MIP robustness and recyclability are successfully evaluated over 6 cycles. Multistep approaches, using MIP alone or in combination with organic solvent nanofiltration (OSN), are discussed aiming to minimize API losses with removal of GTI to reach the threshold of toxicological concern (TTC) for two case studies.
© 2016 Elsevier B.V. All rights reserved.

1. Introduction

In recent years, pharmaceutical regulatory authorities have shown increased concerns about impurities – especially genotoxic impurities (GTI) – in active pharmaceutical ingredients (API) due to their adverse effects on human health [1,2]. Sources for organic impurities in the APIs include unreacted starting materials and reagents, intermediates, catalysts, by-products, reagents and degradation products, as extensively reviewed elsewhere [3]. When the formation of GTIs in APIs production cannot be prevented, purification of the APIs must be performed until the GTI is removed to satisfying levels. Conventional separation techniques used in API purification include crystallization, filtration, distillation, the use of adsorbents, resins and column chromatography [2,3]. Recently, the use of organic solvent nanofiltration (OSN) has also been suggested to address this challenge [4,1]. Another possibility involves the use of molecularly imprinted polymers (MIPs), which explores the formation of selective binding sites in polymers to target molecules by using a molecular template [5,6]. MIPs are reported to be robust, insoluble in most media, obtained by easy synthetic methods and have good reusability [7]. These imprinted polymers have been developed as selective materials for several applications on sensors [8], drug delivery systems [9], solid phase extraction [10], chromatography [11,6] and more recently for the removal of potential GTIs from APIs [12,13]. MIPs also have been suggested to be used in an API polish step after removal of 1,3-diisopropylurea by OSN permeation, to remove residual amounts of this urea from the retentate solution [14]. The current study addresses an industrial challenge in the synthesis of Mometasone furoate (Meta), which is the removal of a genotoxic reactant, 4-dimethylaminopyridine (DMAP), used in one of the final steps of this API production. The current study is focused on the removal of DMAP and the research approach taken consists on the use of a synthetic solution prepared by dissolving Meta and DMAP at known concentrations. However, this approach does not consider additional challenges when translated to an industrial setting due to the potential presence on solution of other species, potentially carried out from previous stages, by-products formed or traces of unreacted reagents, which can affect the specificity of the GTI removal.

Meta is a glucocorticoid steroid used topically to reduce inflammation on skin (eczema, psoriasis) or airways (allergic rhinitis, some asthma patients) pathologies [15,1]. The preparation of a

* Corresponding author.
E-mail address: frederico.ferreira@ist.utl.pt (F.C. Ferreira).

http://dx.doi.org/10.1016/j.seppur.2016.01.053
1383-5866/© 2016 Elsevier B.V. All rights reserved.

MIP for specific removal of DMAP from a Meta solution in DCM was yet to be developed and inhere is identified the conditions that maximize selectivity of an methacrylic acid based MIP not only in identification of polymerization conditions used in its synthesis, but also in the operations conditions to carry out to remove DMAP. Therefore, a systematic study was followed to select the best conditions to develop a MIP for specific binding of DMAP, using this GTI as the template in the imprinting cross-linking polymer process (Fig. 1); a DoE was applied for the selection of the best key variables for the GTI removal, and; a multi-step approach using either MIPs alone or in combination with OSN was quantitatively discussed for a rational process design aiming to minimize API losses, while reaching the threshold of toxicological concern (TTC).

2. Materials and methods

2.1. Materials

Methacrylic acid (MAA), ethylene glycol dimethacrylate (EGDMA) and 4-dimethylaminopiridine (DMAP) were purchased from Acros (Belgium). Dichloromethane (DCM), methanol (MeOH), and hydrochloric acid (HCl) were purchased from Fisher Chemicals (USA). 2,2′-azobis(2-methylpropionitrile) (AIBN) was purchased from Fluka (Switzerland). Acetonitrile (ACN) and formic acid solution was purchased from Aldrich (Switzerland). Mometasone furoate (Meta) was kindly provided by Hovione FarmaCiencia SA (Portugal). All chemicals were of reagent grade or higher and were used as received.

2.2. Apparatus and analysis

Specific surface area and pore diameter of the polymeric particles were determined by nitrogen adsorption according to the BET method. An accelerated surface area and porosimetry system (ASAP 2010 Micromeritics) was used under nitrogen flow. FTIR spectra were recorded as KBr pellets on a Nicolet 6700 spectrometer in the 400–4000 cm^{-1} range using 2 cm^{-1} resolution. Visualization of the morphology of the polymeric particles was performed using scanning electron microscopy (SEM) on a FEG-SEM (Field Emission Gun Scanning Electron Microscope) from JEOL, model JSM-7001F, with an accelerating voltage set to 15 kV. Samples were mounted on aluminum stubs using carbon tape and were gold/palladium coated on a Southbay Technologies, model Polaron E-5100. HPLC measurements were performed on a Merck Hitachi pump coupled to a L-2400 tunable UV detector using an analytic Macherey-Nagel C18 reversed-phase column Nucleosil 100–10, 250 × 4.6 mm, with a flow rate of 1 mL min^{-1} and UV detection at 280 nm; eluents, A: aqueous 0.1% formic acid solution, B: ACN 0.1% formic acid solution; method: 0–3 min, 60–20% A; 3–4 min, 20% A; 4–8 min, 20–60% A; 8–15 min 60% A.

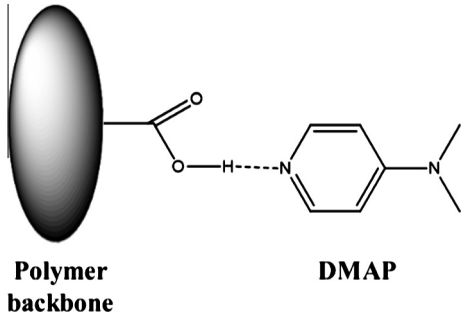

Fig. 1. Predicted hydrogen bond interaction between the functional monomer methacrylic acid (MAA) and the template 4-dimethylaminopyridine (DMAP) in the polymer backbone structure.

2.3. Preparation of polymers

Polymer compositions can be found in Table 1. The model GTI (DMAP) was used as template in the preparation of MIPs, but absent in the preparation of the control polymer labeled as non-imprinted polymer (NIP). The synthesis of MIPs is described below, with quantities exemplified for **MIP2** preparation. MAA (2.323 mmol, 197 μL) was dissolved in DCM (4.35 mL), which works as the porogen. For MIP preparation, the DMAP template (0.581 mmol, 0.071 g) was added to the MAA solution and left stirring for 5 min. EGDMA cross-linker (11.620 mmol, 2.20 mL) and the initiator AIBN (1% wt of total monomers) were added to the polymerization solution, which was purged with a flow of nitrogen for 5 min. The glass tubes were closed and the polymerization was initiated by placing the tubes at 40 °C for 12 h, the temperature was then increased, in increments of 5 °C/30 min, until 65 °C, temperature at which the tubes were left for additional 4 h (method 1). Alternatively, the polymerization was performed isothermally at 65 °C for 16 h (method 2). After polymerization, a white solid was obtained, the tubes were opened and the polymers gently crushed in a mortar. The polymers obtained were washed in a Soxhlet-apparatus with a solution of 0.1 M HCl in MeOH for 48 h for extraction of the template followed by washing with MeOH for 24 h, then the polymers were dried in an oven overnight at 40 °C. The polymers were then grounded in a mechanical mortar and sieved (Resh stainless steel sieves), and the fraction 38–63 μm was used for polymers binding performance evaluation, as well as chemical and morphological characterization. Quantitative analysis of the washing and extraction steps indicated virtually complete template removal. Conditions used are resumed in Table 1.

2.4. Batch binding experiments

Batch binding experiments were evaluated placing 25 mg/mL and 50 mg/mL of each polymer in a 1.5 mL of a 100 and 1000 ppm DMAP solution in DCM in independent vials, which were sealed and stirred for 24 h. The same procedure was performed for a DCM solution of 10 g/L of Meta spiked with 100 ppm of DMAP, as representative solute concentrations and solvent of a post-reaction solution. Binding isotherms and kinetic experiments were performed similarly with a load of 50 mg/mL of **MIP2** stirred in 1.5 mL of DMAP solutions in DCM. Solutions of DMAP with different initial concentrations (5–1000 ppm) were used for 24 h equilibrium experiments to estimate the isotherm. Initial solution of a fixed 100 ppm DMAP concentration was used for kinetic experiments, supernatant samples were taken at 5 min, 15 min, 30 min and at 1, 2, 4, 6, 8, 24 and 33 h and analyzed by HPLC. Experiments to set-up and validate DoE were performed similarly for 24 h using **MIP2** quantity and DCM solutions with DMAP concentrations and volume as reported in the next section. All these sets of experiments were carried out at 60 rpm and 25 °C.

Table 1
Polymer compositions: T – template, MAA – functional monomer, and EGDMA – cross-linker.

	Stoichiometry (mmol)			
	MAA	EGDMA	T	Method
MIP1	0.4	1	0.1	1
MIP2	0.4	2	0.1	1
MIP3	0.4	4	0.4	1
MIP4	0.4	4	0.4	2

After collection, the supernatant was filtered through syringe filters and analyzed by HPLC. The assays were all carried out in duplicates against controls. DMAP bound to the polymer, acting as a scavenger, was calculated from the equation given in (1).

$$q_e = \frac{V[C_0 - C_e]}{M} \quad (1)$$

where q_e (mg/g) is the amount of DMAP bound to the scavenger, C_0 (ppm) is the initial DMAP concentration, C_e (ppm) is the equilibrium concentration of DMAP in solution, V (L) is the volume of solution used and M (g) is the scavenger mass.

2.5. MIP recyclability

MIP samples were regenerated by washing in a Soxhlet-apparatus with a solution of 0.1 M HCl in MeOH for 24 h followed by washing with MeOH for further 24 h, and then the polymer was dried in an oven overnight at 40 °C.

2.6. Experimental design

A two level face-centered cube design (FC-CD) was performed for three input factors: GTI concentration, MIP quantity and solution volume. Table 2 lists the value of each factor.

This FC-CD was composed by 16 runs: 8 factorial points, 2 replicated center points (that provide an estimation of the experimental error) [16] and 6 axial points. A second order model was obtained by fitting the experimental data to Eq. (2).

$$y = K + \beta 1(x_1) + \beta 2(x_2) + \beta 3(x_3) + \beta 1,2(x_{1,2}) + \beta 1,3(x_{1,3}) + \beta 2,3(x_{2,3}) + \beta 1,1(x_1)^2 + \beta 2,2(x_2)^2 + \beta 3,3(x_3)^2 \quad (2)$$

where y is the response measured (DMAP binding by **MIP2**), βi are the regression coefficients corresponding to the main effects, $\beta i,j$ are the coefficients for the second order interactions and $\beta i,i$ are the quadratic coefficients.

The determination of the regression coefficients followed a sequential backward elimination procedure, where the least significant terms ($p > 0.05$) of Eq. (2), in each step, were eliminated and absorbed into the error. Nevertheless, in the case of significant second order interactions or quadratics coefficients, the eliminated terms corresponding to the main effects were reintroduced in the model, but only if lack-of-fit test remained non-significant ($p > 0.05$). The model containing all main factors (x_1, x_2, ...) and all possible interactions (x_1^2, x_1x_2, x_1x_3, x_2^2, ...) was fitted using the software Statistica. The statistical significance of all factors was then evaluated by an analysis of variance (ANOVA) using a Fisher statistical test. A p-value less than 0.05 was considered statistically significant.

2.7. Solid phase extraction experiments

Solid phase extraction (SPE) experiments were performed on Visiprep DL Vacuum Manifold equipped with 3 mL cartridges from Supelco (Germany) that were packed with 50 mg of the selected MIP between Teflon frits. 5 mL of the loading solution was added to the polymer and the eluted solution analyzed by HPLC as described before.

Table 2
Values of each variable of the central composite design.

Factor	Low level (−1)	Central point (0)	High level (+1)
x_1 DMAP (ppm)	7	100	600
x_2 MIP (mg)	37.5	75	100
x_3 Volume (mL)	1.5	3	5

2.8. OSN experimental setup

GMT-oNF-2 membrane was purchased from Borsig Membrane Technology GmbH, Germany. In these experiments 500 mL of a solution with 10,000 ppm of API and 1000 ppm of DMAP in DCM was used. The METcell Cross-Flow System (Evonik MET) comprising high-pressure filtration cells, a tank base and a gear pump was used to carry out the cross-flow filtrations. The diafiltration operation mode, the number of diavolumes, the membrane rejections, the API loss, the GTI removal, and the solvent flux were determined according to methodology published elsewhere [1].

3. Results and discussion

3.1. MIP selection for GTI removal

The first main objective of this study is to develop an effective MIP for specific DMAP binding, for which it was selected inexpensive materials: (i) methacrylic acid, used as functional monomer to provide a carboxyl group for interaction with the target molecule (Fig. 1), and (ii) ethylene glycol dimethacrylate used to provide a polymeric cross-linked structure. The conditions used for synthesis of DMAP imprinted polymers are summarized in Table 1. Different relative molar ratios of the components present in the polymer assembling mixtures were assessed in batch binding experiments (see Fig. 2).

3.1.1. Effect of initial GTI concentration and MIP load

The MIP with higher specific binding for the GTI, DMAP was selected through preliminary tests using DCM solutions at two different DMAP concentrations and MIP mass loads. The two initial DMAP concentrations selected for these studies, 1000 ppm and 100 ppm, are representative, respectively, of (i) a post-reaction in our case study and (ii) a solution from which 90% of DMAP was removed using another process previously to MIP stage, e.g. OSN as previously reported [1].

DMAP binding to the MIPs are higher when this GTI is loaded at lower concentrations (100 ppm) for any of the prepared MIPs. These observations are aligned with previous results [1,17] for removal of a potential GTI, 1,3-diisopropylurea by a similar MIP loaded at 50 mg/mL, which was 90%, but only about 50%, respectively from a 100 ppm and 1000 ppm initial potential GTI solutions. This trend is expected, as higher load GTI concentrations tend to saturate the available binding sites. This effect will be further discussed considering GTI isotherm curve and DoE experiments. Still, it is important to highlight that 78% DMAP removal (condition 50 mg/mL of **MIP2**) from a 1000 ppm GTI solution is significantly higher than the value

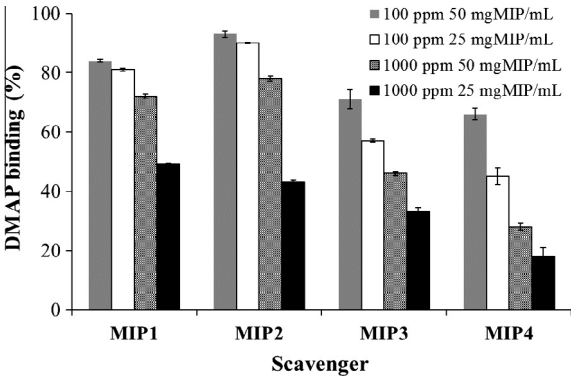

Fig. 2. Specific binding of DMAP in the MIP scavengers. DCM solutions of 100 and 1000 ppm of DMAP were loaded on 25 and 50 mg/mL of scavengers (38–63 μm).

obtained for 1,3-diisopropylurea; allowing to envisage a possible multi-step process using MIPs alone for API degenotoxification.

Additionally, for improved GTI removal we studied two MIP loads, 50 mg/mL and 25 mg/mL, for both DMAP concentrations of 100 and 1000 ppm, translated in degenotoxifications performed at two different MIPs to GTI loads. GTI binding increases as more MIP is used corresponding to a higher availability of binding sites for GTI molecules. Such difference is less stringent for the more efficient polymers, **MIP1** and **MIP2**, at the lower 100 ppm DMAP concentrations; at higher MIPs to GTI loads, implying higher number of binding sites are available for GTI binding.

3.1.2. Effect of stoichiometry and conditions used in the polymerization

MIP1, **MIP2** and **MIP3** were prepared with increasing cross-linker to functional monomer (EGDMA/MAA) molar ratios at values of 2.5, 5.0 and 10.0 using method 1. The role of the cross-linker is to fix the functional groups of MAA around the imprinted molecule and form a highly cross-linked rigid polymer with cavities of complementary shape to the template molecule. After removal of the template, the formed cavities will provide improved recognition of the target molecule. According to the literature, when the dosage of cross-linker is low, such as in the case of **MIP1**, the polymer cannot maintain a stable cavity configuration because of the low cross-linking degree [6]. Indeed, increasing the EGDMA/MAA molar ratios from 2.5 to 5.0 the DMAP binding for a 100 ppm solution increased from 84% for **MIP1** to 93% for **MIP2** when we used 50 mg/mL of the polymer. On the other hand, a high cross-linker dosage confers too much stiffness to the polymer, not being able to adjust to the binding sites. This is probably what happens for **MIP3**, with a higher cross-linker degree and only 71% of binding, when compared to **MIP2** (93%). Note however that the template to functional monomer molar ratio was 0.25 to **MIP1** and **MIP2** and 1.0 for **MIP3** and **MIP4**. Whereas the molar ratio of MAA/EGDMA most probably plays the major role on GTI binding, the template to functional monomer molar ratio is also a key factor for MIP performance. DMAP catalyses the methanesulfonylation reaction of the Meta precursor with mesyl chloride (MsCl). MsCl, in the presence of alcohols, can generate sulfonate ester species, which are known to attack the DNA. Therefore removal of unreacted MsCl and resulting sulfonate esters is also crucial. In the current study, MIPs with a lower template to functional monomer molar ratio (**MIP1** and **MIP2**) present higher GTI removals. It has been described that this ratio has influence on the number of binding sites available and also for high values the non-specific binding capacity is favored, lowering the binding selectivity [6]. The presence of a higher crosslinker ratio in **MIP3** formulation lowers the number of affinity binding sites due to the stiffness of the polymer, which does not allow the cavities around the template to properly adjust during polymerization [18].

The polymerization reaction conditions used also influence the GTI binding. Whereas **MIP1**, **MIP2** and **MIP3** polymerization was carried out with a gradient of temperature, **MIP4** was prepared isothermally at 65 °C for 16 h (method 2) at the same stoichiometry of **MIP3**, i.e. at an EGDMA/MAA molar ratio of 10. The results suggested that the temperature gradient allows a better polymeric chain adjustment on the creation of the binding cavities for molecular recognition, resulting on a worse binding performance by **MIP4**.

3.2. *MIP2* performance and characterization

*3.2.1. Performance of the **MIP2***

From the four MIPs prepared, **MIP2** exhibit the best performance and therefore it was selected for further studies within this work. This MIP was produced with a molar ratio of 1:4:20 for template:monomer:cross-linker, which is also described in the literature as a typical arrangement for a MIP preparation [5].

A non-imprinted polymer, **NIP2**, was prepared using the same component molar ratio of 1:4:20 (T:MAA:EGDMA) and assessed for GTI removal from a 100 ppm solution of DMAP loaded on 50 mg/mL of scavenger (38–63 μm) for testing in batch binding experiments. The high DMAP binding in NIP can be attributed to the interactions between the amine groups of DMAP and the carboxylic groups of MAA. However. the percentage of DMAP binding was even higher for the imprinted polymer **MIP2** (93%) when compared with the respective non-imprinted polymer **NIP2** (75%) showing that the introduction of the template molecule, during the preparation of **MIP2** has a significant impact on the selectivity of the polymer toward it, most probably due to favorable geometric presentation of the carboxylic groups and DMAP positioning within the MIP matrices. The additional 18% of specific DMAP binding for **MIP2**, compared to **NIP2**, makes **MIP2** a suitable scavenger for this GTI.

In the context of API purification, for the pharmaceutical industry, this gain in selectivity has a high economic impact. **MIP2** degenotoxification potential was assessed in batch binding experiments for a mixture of 10 g/L of Meta spiked with 100 ppm of DMAP in DCM at a MIP load of 50 mg/mL. A 93% of DMAP was removed from the solution, but 12% of the Meta was also non-specifically bound to the MIP, which is a significant API loss. Still these results represent a dramatic decrease in the amount of GTI to API, starting from an initial ratio of 10 reaching a final ratio of 0.8 mgDMAP to gMeta. Note that 0.8 mgDMAP to gMeta is remarkable close of the lower TTC established at a value of 0.75 mgDMAP/gMeta when Meta is applied to manage skin related inflammation; for the same API losses, a DMAP removal of 93.4% will meet the required TTC. The API losses obtained are significantly high and further SPE experiments were performed to reduce such value. Such results will be further discussed in the context of acceptable TTC values. Moreover, the binding for DMAP, on the presence of a 100 fold mass excess of Meta, was a similar value to the one found in the absence of Meta, establishing that binding of DMAP to **MIP2** is independent of the API concentration.

*3.2.2. Characterization of the **MIP2***

The selected **MIP2** and **NIP2** were further characterized by FTIR, BET and SEM. FTIR spectra of the polymers (Fig. 3) showed the characteristic peaks of carboxylic acids (from the MAA functional monomer) corresponding to the strong and broad band for the O—H stretch in the region 3200–2800 cm^{-1}, centered at about 3000 cm^{-1}. The carbonyl stretch C=O, from the saturated and unsaturated aliphatic esters, from the EGDMA cross-linker and the MAA carboxylic group corresponds to the intense band at 1750 cm^{-1}. The typical carboxylate C—O stretch (1300 cm^{-1}) and O—H bends

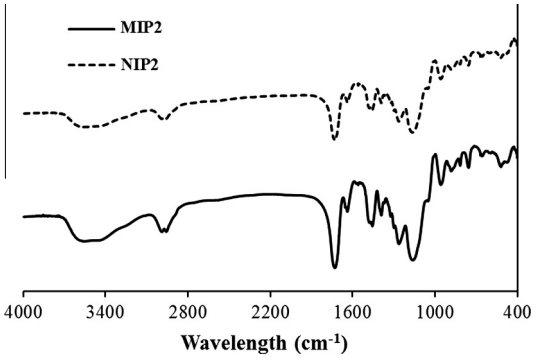

Fig. 3. IR spectra in KBr of **MIP2** and **NIP2**.

(1430, 950 cm^{-1}) were also observed. The similarity between the spectra of **MIP2** and **NIP2**, and the absence of characteristic peaks corresponding to the GTI molecule, suggests complete removal of the template molecule.

According to the results for BET analyses presented in Table 3, **MIP2** presents a lower surface area and lower average pore diameter than **NIP2** which supports the idea that the higher DMAP adsorption for **MIP2** (93%) than **NIP2** (75%), is due to a specific interaction process and not due to higher surface area for adsorption in the MIPs [19]. No significant differences were found between **MIP2** and **NIP2** polymers on SEM images presented in Fig. 4, depicting the morphologies with agglomerates of smooth surfaced nanoparticles.

MIP2 *recyclability* proved to be robust without loss of selectivity for the GTI. After binding assays, MIP washing with 0.1 M HCl in MeOH solution allows to remove the template and reuse the MIP in further DMAP removal. The DMAP binding remained fairly constant ~94% and similar to the initial value of 93% over 6 assays performed. The possibility to recycle a MIP scavenger without efficiency loss is crucial from an industrial point of view.

3.3. GTI removal by ***MIP2*** as a function of key variables

3.3.1. Design of experiments

For further study of the effect of DMAP concentration vs MIP quantity load into DMAP removal, a statistical experimental design was performed. A face-centered cube design (FC-CD) was devised to characterize the effect of GTI concentration (x_1, ppm), MIP quantity (x_2, mg) and solution volume (x_3, mL) on the percentage of binding (%), used as response variable. Details of the design and the experimental results are given in Table 4.

The outcome of the ANOVA can be visualized in a Pareto chart (Fig. 5), in which the absolute value of the magnitude for the standardized estimated effect (the estimate effect divided by the standard error) of each factor is plotted in decreasing order and compared to the minimum magnitude of a statistically significant factor with 95% of confidence ($p = 0.05$), represented by the vertical red dashed line.

The Pareto chart shows DMAP concentration is the variable with greatest impact on the quadratic function for the GTI binding, followed by the interaction between the DMAP concentration with MIP quantity and solution volume. The factors not statistically significant at confidence level of 95% were pooled into the error term and a new reduced model was obtained using only the significant factors for the new regression, described by Eq. (3).

$$\text{Binding } (\%) = 48.72 + 0.42x_1 - 0.001x_1^2 + 0.05x_2 + 0.66x_3 + 0.001x_1x_2 - 0.02x_1x_3 \quad (3)$$

In the ANOVA analysis (Table 5) performed on the reduced model a lack-of-fit test, which compares the residual error (i.e., the error associated with the fitted model) to the pure error from replication at the central point, was also evaluated and in this case, a *p*-value higher than 0.05 was obtained, stressing that the model is statistically significant. For the binding, an *R*-square value of 0.98431 was obtained indicating a good response between the model and the experimental results.

Table 3
Physical properties of **MIP2** and **NIP2**, obtained by multipoint BET method.

	BET surface area ($m^2\ g^{-1}$)	Pore volume ($cm^3\ g^{-1}$)	Average pore diameter (nm)
MIP2	207	0.024	5.6
NIP2	242	0.025	7.3

The area contours for binding percentage as function of GTI concentration and MIP quantity (Fig. 6A) and of GTI concentration and volume of solution (Fig. 6B) were calculated using the reduced model expressed by Eq. (3).

The high GTI binding yields were obtained for DMAP concentrations in the range 250–350 ppm, for 100 mg of **MIP2** and 1.5 mL of GTI solution. The highest binding value of 95% was found at a DMAP concentration of 285 ppm (Table 6), which is close to the value found experimentally for a 100 ppm solution at a **MIP2** load of 50 mg/mL; indicating a probable saturation of **MIP2** binding sites, since for a higher MIP quantity (66.7 mg/mL) the gain in GTI binding is not significant. To confirm this trend a complete isotherm was experimentally evaluated at 50 mg/mL and 1.5 mL volume, varying the DMAP initial concentration (Fig. 7) in which we can observe the binding saturation to happen around the range of concentration values obtained from the statistical model, 250–350 ppm. Moreover, the binding percentages for the best values of 100, 259 and 307 ppm of DMAP solution with 75 mg of **MIP2** and 285 ppm of DMAP with 100 mg with 1.5 mL of solution is also reported in Table 6.

3.3.2. Equilibrium and kinetic of DMAP binding to ***MIP2***

The adsorption isotherm for DMAP by **MIP2** is shown in Fig. 7. The top panel shows the DMAP binding percentage as function of the initial DMAP solution concentration. As described in the preliminary results there is a decrease in DMAP binding percentage to the MIP with increase of DMAP concentration from 100 to 1000 ppm in the starting solution is used, which is most probably related with a decrease in the proportion of available binding sites in the polymer to the candidate solute molecules to binding, still as illustrated in the isotherm curve shown in the middle panel, polymer binding saturation was not completely reached within the range of DMAP concentrations tested. For an initial DMAP concentration below 256 ppm, there is a decrease on binding efficiency with decrease on DMAP concentrations, which is typical of adsorption processes, therefore to establish the type of isotherm followed the experimental data were fitted to different mathematical models of adsorption. The correlation coefficients for the Freundlich plot at a value of 0.9467 is higher than for the Langmuir plot at a value of 0.8213, showing that DMAP adsorption by **MIP2** follows the Freundlich model at room temperature (Fig. 7). This model assumes that as the DMAP concentration increases, the concentration of the GTI on the MIP surface will increase also [20]. Additionally, this model is indicative that we are in the presence of a heterogeneous binding site distribution which is one of the characteristics of polymers obtained by bulk polymerization [5,6]. The physical parameters determined for the theoretical binding models are included in the supporting information. Additionally, the kinetics of binding between **MIP2** and DMAP was evaluated for an initial solution of 100 ppm establishing that the binding process is very fast reaching the maximum 93% of GTI binding in less than 5 min, which remains constant over the next 33 h.

3.4. SPE experiments and process design for API purification

3.4.1. SPE experiments

A significant fraction of Meta (1.2 g/L) was non-specifically bound by **MIP2** in batch binding experiments. In order to promote specific over non-specific binding, and prevent significant Meta losses, we performed studies employing SPE with a **MIP2** load of 50 mg to 5 mL DCM, i.e a MIP load of 10 mg/mL. In such experiments, from solutions of 10 g/L of Meta and 100 ppm of DMAP, 0.4 g/L of Meta were lost. However, the percentage of DMAP binding was also lower to a value of 88% rather than the 93% obtained for the batch experiments. Overall, in the SPE experiment the contamination of Meta was decreased from 10 mgDMAP/gMeta to

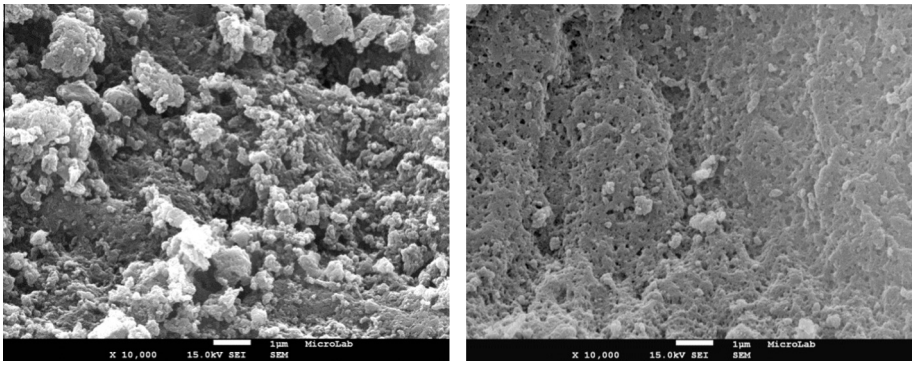

Fig. 4. SEM images of **MIP2** (left) and **NIP2** (right) polymer particles.

Table 4
GTI binding percentage for each experiment of the central composition design.

Exp.	x_1	x_2	x_3	Binding (%)
1	7	37.5	1.5	52.69
2	7	37.5	5	61.17
3	7	100	1.5	59.09
4	7	100	5	57.72
5	600	37.5	1.5	66.02
6	600	37.5	5	22.78
7	600	100	1.5	93.94
8	600	100	5	60.25
9	7	75	3	55.43
10	600	75	3	67.34
11	100	37.5	3	80.36
12	100	100	3	92.83
13	100	75	1.5	93.50
14	100	75	5	86.02
15	100	75	3	91.10
16	100	75	3	90.71

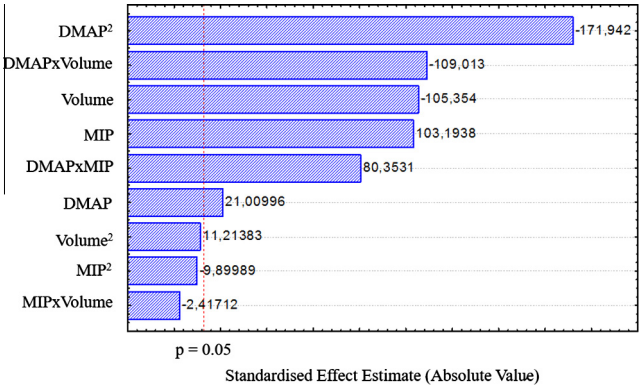

Fig. 5. Pareto chart for the standardized effects of the variables DMAP (x_1), MIP (x_2) and volume (x_3) on the DMAP binding by **MIP2**.

Table 5
Results of the analysis of variance (ANOVA) performed to the model.

	DF	SS	MS	*F*-value	*p*-Value
Error	6	83.37	13.89		
Lack of fit	8	96.70	12.09	158.95	0.0613
Pure error	1	0.076	0.076		

1.25 mgDMAP/gMeta in a single step, whereas a value of 0.8 mgDMAP/gMeta was previously obtained for a single step batch experiment at 50 mgMIP/ml. Nevertheless, SPE experiments were conducted at a MIP load and a GTI to MIP ratio 5 times lower than in the batch experiment. For a more fair comparison, a batch

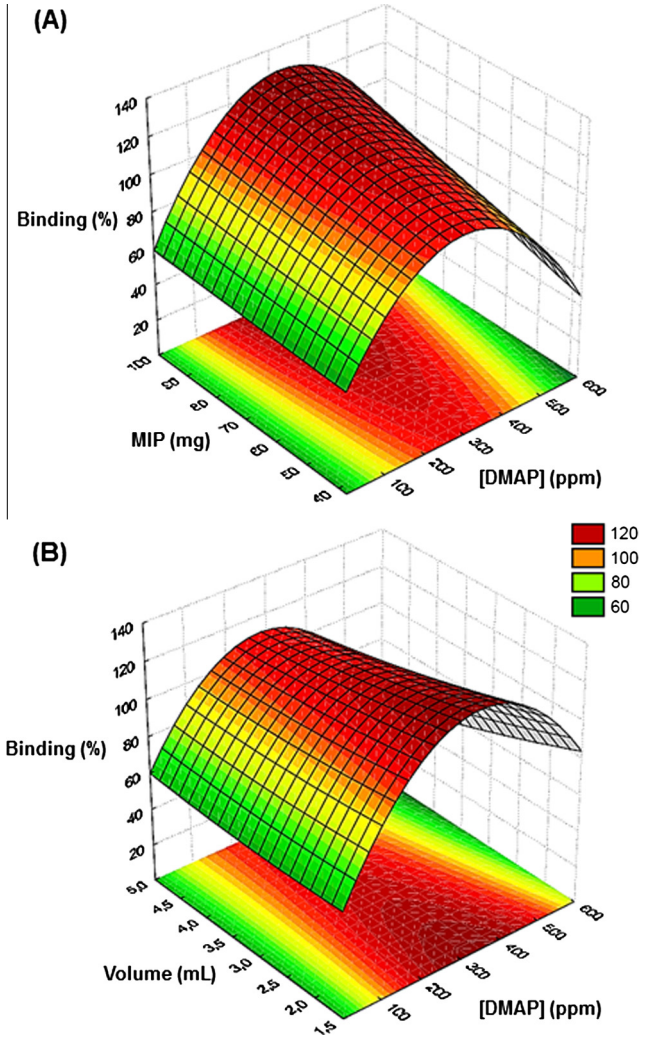

Fig. 6. Response surface plots of the central composite design for the optimization of DMAP binding by **MIP2**. Effect of: (A) DMAP concentration and MIP quantity; (B) DMAP concentration and solution volume on the binding.

Table 6
Validation of the model predictions.

[DMAP] (ppm)	MIP (mg)	Volume (mL)	Binding (%)
285	100	1.5	95
100	75	1.5	93
256	75	1.5	98
307	75	1.5	93

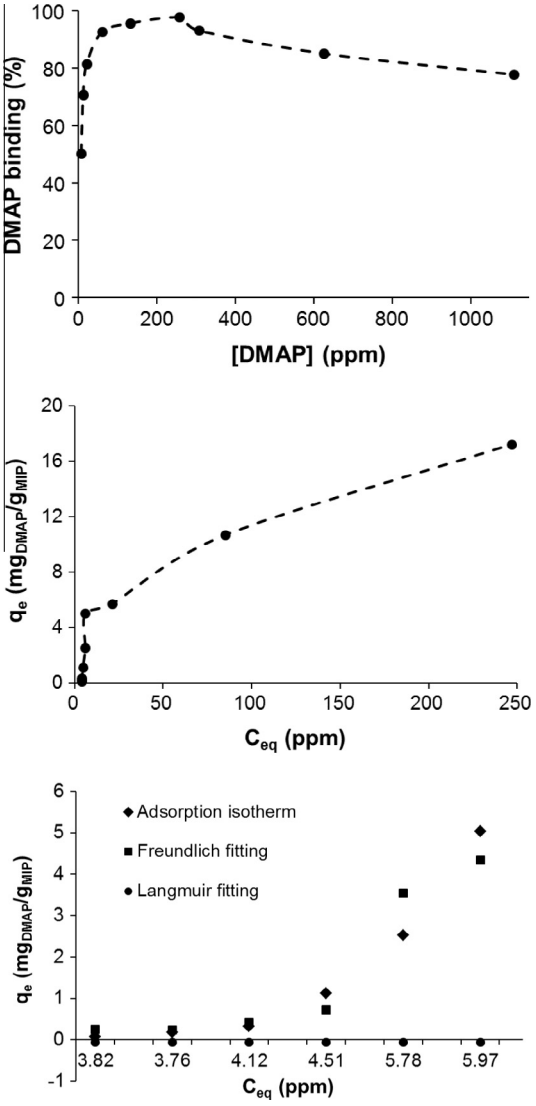

Fig. 7. *Top:* DMAP binding isotherm for **MIP2**. *Middle:* **MIP2** adsorption capacity of various concentrations of DMAP. *Bottom:* Fitting of the DMAP adsorption isotherm to **MIP2** at lower solute concentration range to Langmuir and Freundlich models.

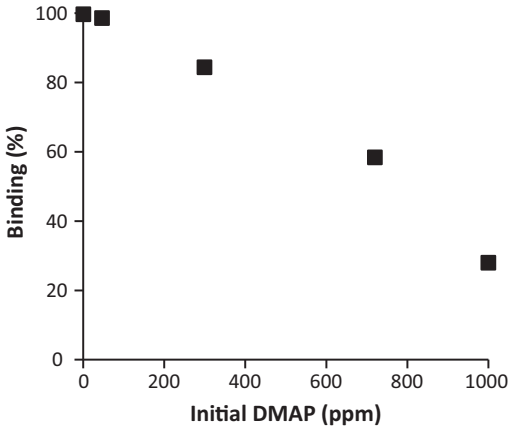

Fig. 8. DMAP binding in SPE experiments for **MIP2**.

experiment with the same MIP load of 50 mg in a 5 mL into a 100 ppm DMAP solution, i.e the same MIP load of 10 mg/mL used in the SPE, was performed in batch. This experiment resulted in a decrease on DMAP binding to 77%, a value lower than the 88% obtained for the SPE experiments in similar conditions and an API loss of 4%, i.e at this lower MIP loading degenotoxification in batch only reach a 2.4 mgDMAP/gMeta limit. Confirming that, compared to batch experiments, SPE operation mode promotes the specific interaction of the MIP toward the GTI and the use of lower MIP load can contribute to minimize the API losses. This is the reason why we decide to maintain the ratio of 50 mgMIP/mL and increase the solution volume to 5 mL. The percentage of DMAP binding as function of the initial DMAP concentration for a 10 mgMIP/ml load for a SPE operation is presented in Fig. 8, with GTI removal by the MIP being significantly more efficient at lower GTI concentrations.

3.4.2. Process design for API purification

The amount of GTI allowed in APIs is determined considering an acceptable TTC value of 1.5 μg/day and the maximum daily dose (g/day) [21]. In here, two case scenario are considered, the intake of a maximum daily dosage of 200 μg and 2 mg of Meta, respectively, to reduce inflammation on airways and skin; which represents a degenotoxification of API to reach 7.5 and 0.75 mgGTI/gAPI limits. Considering the results discussed in the previous section, the SPE experiments were performed with a 10 mgMIP/mL load which much probably is suboptimum concerning DMAP removal, but offers lower API losses. Therefore, the challenge in the multistep process design is to reach the degenotoxification levels targeted with the minimal losses in API. In a first approach, 5 successive steps of DMAP removal by MIP were performed and the results obtained are represented in Fig. 9. API recovery decreases over each step, being required 4 (1.7 mgGTI/gAPI) or 5 (0.4 mgGTI/gAPI) steps to comply with the thresholds established for the airways (7.5 mgGTI/gAPI) or skin (0.75 mgGTI/gAPI) inflammation management case study studies, respectively. However, such results were only achieved at a high significant losses of API between 16% and 20%, considering this values a strategy of single step increasing the MIP load could be more efficient. Recall that in a single batch step using a MIP load 5 times, a limit of 0.8 mgDMAP/gMeta was previously obtained, with 12% API losses.

The results in Fig. 8 clearly show the inefficiency on MIP binding of the SPE operation at DMAP at high concentrations with only 28% DMAP binding. The first steps applied to remove the DMAP at high concentration penalize overall API efficiency without a significant gain in GTI removal. In the SPE multistep operation, i.e. using MIP alone, to reach the limits aimed, 7.5 and 0.75 mgDMAP/gMeta, it is required at least 4 or 5 steps (Fig. 9 top panel). Consequently, the cumulative losses in API become significant with at values of 16% and 20%, respectively. The use of OSN diafiltration approach for removal of GTI from API was previously established [4] and applied to separation of DMAP from META [1] in a comparative study with other conventional technologies, such as recrystallization. In such study was assessed the efficiency on DMAP removal and Meta losses as a function of diavolumes used, establishing higher GTI removal over API losses for the first four diavolumes, but lower incremental performance for subsequent diavolumes. Therefore, considering higher performance for the first diavolumes of OSN at higher DMAP concentrations and higher DMAP removal at lower concentrations for MIPs operations; it is here assessed quantitatively a multistep process consisting of first x diavolumes, followed by y-steps of MIP–SPE operations on a total $(x + y)$ of 5 steps. The results obtained are presented in Fig. 9 (bottom panel), where it is shown that the use of OSN alone at 5 diavolumes (x: y = 5:0) provides a route for Meta degenotoxification minimizing API losses, which is sufficient for Meta dosages associated with airways inflammation therapies (requirement of 7.5 mgDMAP/gMeta), but not when Meta is intend to be used in for skin

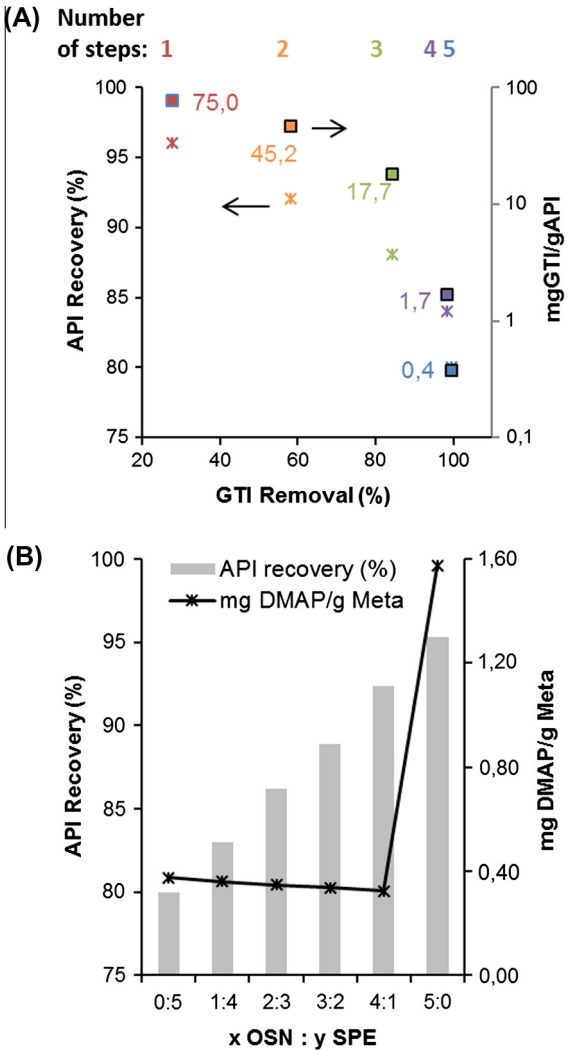

Fig. 9. Performance of a multistep process concerning DMAP removal, Meta losses and level of degenotoxification of DMAP to Meta limit reached for (A) 5 successive SPE steps using MIP alone (top panel) and (B) combining OSN and MIP operations in *x* diavolumes and *y* SPE steps, respectively (bottom panel).

inflammation (requirement of 0.75 mgDMAP/gMeta). On the other hand the use of MIPs-SPE in 5 steps process, alone or in combination with OSN, always fulfill the requirements for both airways and skin inflammation (degenotoxification reaches a ratio below of 0.75 mgDMAP/gMeta). Still the use 5 steps of MIP–SPE alone implies a significant API loss (20%), which can be mitigated using the OSN diafiltration, reaching a value 7.6% of API losses of in the case of using a diavolume of 5 followed by a single MIP–SPE (x:y = 5:1). Note that OSN has been suggested to be used in the context of pharmaceutical industry not only for degenotoxification [4], but also for direct recovery of APIs [22–24] or for recycling catalysts [25,26] and chiral resolving agents [27,28].

The use of solvent intensive processes poses additional environmental concerns, a preliminary estimation of DCM use points out for values of 530–670 kgDCM/kgMeta for 4–5 SPE–MIP purification steps, respectively, when MIPs were used alone; and 800 kgDCM/kgMeta for a multistep process when a OSN diafiltration stage of 5 volumes precedes 1 MIP polishing step. These values are based in laboratory data where 10 g/LMeta, while 36.6 g/LMeta [15] are used industrially, therefore solvent use per Kg of API is overestimated at least by a factor of 3.6. Note that solvent use estimated fall within the range of application of chromatographic methods for some API purification, in which elutant can reach 1000 L per kg of API in a first chromatographic step [29], with API being later concentrated for further purification steps. These values are all extremely high and solvent recycling in place by distillation of DCM, a low boiling point, is highly recommended. Alternatively, and in particular for solvents of higher boiling points, there is a call for implementations of low solvent intensity methodologies, such as cascade chromatography [30], OSN-chromatographic hybrid processes with solvent recycling [31] or membrane processes for solvent recycling [32,33].

Moreover, considering an OSN diafiltration of 5 diavolumes followed by 1 SPE–MIP, in the experimental conditions used, would be needed 1:1 mass equivalent of MIP for Meta recovered. This value is lower than the reported for resin based separations which are higher than 20:1 for a resin:API ratio [34–36]. Still it points out for the need to recycle the MIP, which in the current work was shown over 6 recycles without decreasing its binding performance for DMAP.

4. Conclusion

The potential use of molecular imprinted polymers prepared from MAA as functional monomer for the effective removal of DMAP from an API solution was investigated. The conditions that yield a MIP with higher binding affinity to DMAP are the ones used on the preparation of **MIP2**, where a MAA:EGDMA:template ratio of 0.4:2.0:0.1 was used and polymerization temperature after an initial plateau for 12 h at 40 °C increases to 65 °C at 5 °C/30 min, at which temperature tubes were left for additional 4 h. Adsorption of DMAP by **MIP2** was found to be effective at room temperature. For **MIP2** DMAP adsorption increased with increasing initial concentration of GTI, reaching equilibrium saturation. Our results show that, even in a typical industrial scenario, where DMAP is present in low concentrations compared to high amounts of API, we have an effective removal of about 93% of DMAP with a DMAP concentration of about 100 ppm. This resulted in a 12% loss of API when present in a 100 fold excess to the GTI due to non-specific binding. However, with **MIP2** operated in an SPE experiment the API loss is reduced to 4% with 88% GTI removal. We proposed a combined strategy of OSN with one **MIP2** stage in SPE operating mode. In this way we can remove more than 99.7% of GTI with a 8% loss of API to reach a final ratio lower than 0.3 mgDMAP/gMeta. DoE experiments revealed a good match with experimental results and the best DMAP/**MIP2**/volume target ratio was determined to maximize GTI binding.

Acknowledgements

The authors thank Professor Carla Nunes for help with FTIR measurements and Professor Filipa Ribeiro (IST) with help with particle fractioning and use of Resh stainless steel sieves equipment. The authors acknowledge dedicated funding for this work from Fundação para a Ciência e Tecnologia/Ministério da Educação e Ciência (FCT/MEC) of the project Genosep (PTDC/QEQ-PRS/2757/2012). Additional funding from FCT/MEC includes, the Principal Investigator Contracts (IF/00915/2014 (TC) and IF/00442/2012 (FCF)) and co-funding for the doctoral Grant SFRH/BDE/51907/2012 (R.V.) from FCT and Hovione. Moreover, the authors acknowledge funding for the R&D units: (i) iBB-Institute for Bioengineering and Biosciences from FCT/MEC (UID/BIO/04565/2013) and from European Regional Development Fund (ERDF), (Programa Operacional Regional de Lisboa 2020, Project Nr. 007317) and (ii) LAQV-REQUIMTE, by national funds, from FCT/MEC (UID/QUI/50006/2013) and from the ERDF (PT2020 Partnership Agreement: POCI-01-0145-FEDER-007265).

Appendix A. Supplementary material

Supplementary data associated with this article can be found, in the online version, at http://dx.doi.org/10.1016/j.seppur.2016.01.053.

References

[1] G. Székely, M. Gil, B. Sellergren, W. Heggie, F.C. Ferreira, Environmental and economic analysis for selection and engineering sustainable API degenotoxification processes, Green Chem. 15 (2013) 210–225.

[2] L. Zhou, B. Mao, R. Reamer, T. Novak, Z. Ge, Impurity profile tracking for active pharmaceutical ingredients: case reports, J. Pharm. Biomed. Anal. 44 (2007) 421–429.

[3] G. Székely, M. Sousa, M. Gil, F.C. Ferreira, W. Heggie, Genotoxic impurities in pharmaceutical manufacturing: sources, regulations, and mitigation, Chem. Rev. 16 (2015) 8182–8229.

[4] G. Székely, J. Bandarra, W. Heggie, B. Sellergren, F.C. Ferreira, Organic solvent nanofiltration: a platform for removal of genotoxins from active pharmaceutical ingredients, J. Membr. Sci. 381 (2011) 21–33.

[5] A. McCluskey, C.I. Holdsworth, M.C. Bowyer, Molecularly imprinted polymers (MIPs): sensing, an explosive new opportunity?, Org Biomol. Chem. 5 (2007) 3233–3244.

[6] L. Chen, S. Xu, J. Li, Recent advances in molecular imprinting technology: current status, challenges and highlighted applications, Chem. Soc. Rev. 40 (2011) 2922–2942.

[7] A.G. Mayes, M.J. Withcombe, Synthetic strategies for the generation of molecularly imprinted organic polymers, Adv. Drug. Deliv. Rev. 57 (2005) 1742–1778.

[8] S. Korposh, I. Chianella, A. Guerreiro, S. Caygill, S. Piletsky, S.W. James, R.P. Tatam, Selective vancomycin detection using optical fibre long period gratings functionalised with molecularly imprinted polymer nanoparticles, Analyst 139 (2014) 2229–2236.

[9] A.L.M. Ruela, E.C. Figueiredo, G.R. Pereira, Molecularly imprinted polymers as nicotine transdermal delivery systems, Chem. Eng. J. 248 (2014) 1–8.

[10] A. Beltran, F. Borrull, P.A.G. Cormack, R.M. Marcé, Molecularly-imprinted polymers: useful sorbents for selective extractions, Trends Anal. Chem. 29 (2010) 1363–1375.

[11] E. Amut, Q. Fu, Q. Fang, R. Liu, A. Xiao, A. Zeng, C. Chang, In situ polymerization preparation of chiral molecular imprinting polymers monolithic column for amlodipine and its recognition properties study, J. Polym. Res. 17 (2010) 401–409.

[12] G. Székely, E. Fritz, J. Bandarra, W. Heggie, B. Sellergren, Removal of potentially genotoxic acetamide and arylsulfonate impurities from crude drugs by molecular imprinting, J. Chromatogr. A 1240 (2012) 52–58.

[13] B. Sellergren, E. Fritz, G. Székely, Polymers for drug purification, WO 2012172075 A1, 2012.

[14] G. Székely, J. Bandarra, W. Heggie, F.C. Ferreira, B. Sellergren, Design, preparation and characterization of novel molecularly imprinted polymers for removal of potentially genotoxic 1,3-diisopropylurea from API solutions, Sep. Purif. Technol. 86 (2012) 190–198.

[15] W. Heggie, J. Bandarra, Process for the preparation of Mometasone furoate, US 6177560 B1, 2001.

[16] R. Leardi, Experimental design in chemistry: a tutorial, Anal. Chim. Acta 652 (2009) 161–172.

[17] G. Székely, J. Bandarra, W. Heggie, B. Sellergren, F.C. Ferreira, A hybrid approach to reach stringent low genotoxic impurity contents in active pharmaceutical ingredients: combining molecularly imprinted polymers and organic solvent nanofiltration for removal of 1,3-diisopropylurea, Sep. Purif. Technol. 86 (2012) 79–87.

[18] J. He, Q. Zhu, Q. Deng, Investigation of imprinting parameters and their recognition nature for quinine-molecularly imprinted polymers, Spectrochim. Acta A 67 (2007) 1297–1305.

[19] M.S. Silva, R. Viveiros, M.B. Coelho, A. Aguiar-Ricardo, T. Casimiro, Supercritical CO_2-assited preparation of a PMMA composite membrane for bisphenol A recognition in aqueous environment, Chem. Eng. Sci. 68 (2012) 94–100.

[20] N.D. Zakaria, N.A. Yusof, J. Haron, A.H. Abdullah, Synthesis and evaluation of a molecularly imprinted polymer for 2,4-dinitrophenol, Int. J. Mol. Sci. 10 (2009) 354–365.

[21] EMEA Guidelines on the "Limits on Genotoxic Impurities", EMEA/CHMP/QWP/251344/2006, 2006.

[22] J. Vanneste, D. Ormerod, G. Theys, D. Van Gool, B. Van Camp, S. Darvishmanesh, B. Van der Bruggen, Towards high resolution membrane-based pharmaceutical separations, J. Chem. Technol. Biot. 88 (1) (2013) 98–108.

[23] J. Geens, B. De Witte, B. Van der Bruggen, Removal of API's (Active pharmaceutical ingredients) from organic solvents by nanofiltration, Separ. Sci. Technol. 42 (11) (2007) 2435–2449.

[24] L. Peeva, J.D.S. Burgal, I. Valtcheva, A.G. Livingston, Continuous purification of active pharmaceutical ingredients using multistage organic solvent nanofiltration membrane cascade, Chem. Eng. Sci. 116 (2014) 83–194.

[25] F.C. Ferreira, L.C. Branco, K.K. Verma, J.G. Crespo, C.A.M. Afonso, Application of nanofiltration for re-use of Sharpless catalytic system in asymmetric di-hydroxylation, Tetrahedron-Asymmetr 18 (2007) 1637–1641.

[26] L.C. Branco, F.C. Ferreira, J.L. Santos, J.G. Crespo, C.A.M. Afonso, Sharpless asymmetric dihydroxylation of olefins in water-surfactant media with recycling of the catalytic system by membrane nanofiltration, Adv. Synth. Catal. 350 (2008) 2086–2098.

[27] N.F. Ghazali, F.C. Ferreira, A.J.P. White, A.G. Livingston, Enantiomer separation by enantioselective inclusion complexation-organic solvent nanofiltration, Tetrahedron-Asymmetry 17 (12) (2006) 1846–1852.

[28] F.C. Ferreira, H. Macedo, U. Cocchini, A.G. Livingston, Development of a liquid-phase process for recycling resolving agents within diastereomeric resolutions, Org. Process. Res. Dev. 10 (4) (2006) 784–793.

[29] S. Garg, A process for the recovery of substantially pure tricyclic macrolide, WO 2005019226 A1, 2005.

[30] Y.-E. Li, Method of purification of rapamycin and its analogs by use of cascade chromatography, EP 2147000 A1, 2010.

[31] C. Pink, E. Rundquist, Use of organic solvent nanofiltration and liquid-liquid chromatography for the recovery of pharmaceutical products, EP 2782652 A1, 2014.

[32] C. Lee, R. Helmy, C. Strulson, J. Plewa, E. Kolodziej, V. Antonucci, B. Mao, C.J. Welch, Z. Ge, M.A. Al-Sayah, Removal of electrophilic potential genotoxic impurities using nucleophilic reactive resins, Org. Process Res. Dev. 10 (2010) 1021–1026.

[33] S. Darvishmanesh, L. Firoozpour, J. Vanneste, P. Luis, J. Degrève, B. Van der Bruggen, Performance of solvent resistant nanofiltration membranes for purification of residual solvent in the pharmaceutical industry: experiments and simulation, Green Chem. 13 (12) (2011) 3476–3483.

[34] J.F. Kim, G. Szekely, I.B. Valtcheva, A.G. Livingston, Increasing the sustainability of membrane processes through cascade approach and solvent recovery-pharmaceutical purification case study, Green Chem. 16 (2014) 133–145.

[35] R. Kecili, J. Billing, M. Leeman, D. Nivhede, B. Sellergren, A. Rees, E. Yilmaz, Selective scavenging of the genotoxic impurity methyl p-toluenesulfonate from pharmaceutical formulations, Sep. Purif. Technol. 103 (2013) 173–179.

[36] R. Kecili, D. Nivhede, J. Billing, M. Leeman, B. Sellergren, E. Yilmaz, Removal of acrolein from active pharmaceutical ingredients using aldehyde scavengers, Org. Process Res. Dev. 16 (2012) 1225–1229.